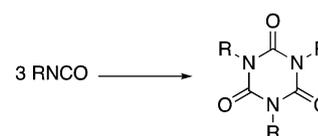## COMMUNICATION

Check for updates

Aluminium-catalysed isocyanate trimerization, enhanced by exploiting a dynamic coordination sphere†‡

Mohammed A. Bahili,[ab] Emily C. Stokes, [ID][a] Robert C. Amesbury,[a]
Darren M. C. Ould,[a] Bashar Christo,[a] Rhian J. Horne,[a] Benson M. Kariuki, [ID][a]
Jack A. Stewart,[a] Rebekah L. Taylor,[a] P. Andrew Williams,[a] Matthew D. Jones, [ID][c]
Kenneth D. M. Harris [ID][a] and Benjamin D. Ward [ID]*[a]

Main-group metals are inherently labile, hindering their use in catalysis. We exploit this lability in the synthesis of isocyanurates. For the first time we report a highly active catalyst that trimerizes alkyl, allyl and aryl isocyanates, and di-isocyanates, with low catalyst loadings under mild conditions, using a hemi-labile aluminium-pyridyl-bis(iminophenolate) complex.

Scheme 1 Trimerization of isocyanates.

Catalytic applications of Earth-abundant main-group metals, such as aluminium, have compelling environmental and economic benefits. In contrast to the extensively-used platinum group metals, they are non-toxic, inexpensive, and readily available;[1] furthermore, the requirement to reprocess the metals *via* complex, expensive, and polluting recycling processes is therefore less critical. However, the widespread use of main group metals in catalysis is hindered by the fact that they often exhibit labile and unpredictable coordination chemistry, leading to ligand redistribution and poorly-defined catalyst species. We demonstrate here that such lability can actually be exploited as a part of the catalyst design to give a dynamic coordination environment that enhances catalytic performance.

Trimerization of isocyanates (RNCO, Scheme 1) is the most rapid, economical and atom-efficient route to isocyanurates, which are used in a diverse range of applications, such as medicines,[2–5] selective anion binding,[6] microporous materials[7,8] and coating materials.[9] However, isocyanurates' principal application is in the construction industry; they are the key component in rigid polyurethane foams which are used ubiquitously as insulation

boards and are responsible for their mechanical and thermo-setting properties.[10]

Isocyanates can be trimerized by amines,[11] phosphines,[12–15] N-heterocyclic carbenes,[16] inorganic salts,[17] phosphides,[18,19] and main group and transition metal complexes,[20–28] but existing catalysts often require high catalyst loadings, high temperatures (*e.g.* ≥100 °C for amines and halides),[11,17] can give a mixture of oligomers, and/or fail to trimerize both alkyl and aryl isocyanates. In this communication we report the first catalyst that excels in all of these aspects, specifically an aluminium complex that selectively trimerizes alkyl, allyl and aryl isocyanates, and di-isocyanates, at mild temperatures, with low catalyst loadings.

Preparation of aluminium complexes. The 6-coordinate aluminium complex [Al(Salpy)(OBn)] (**3**) incorporating the pyridyl-bisimino-phenolate (Salpy) ligand (**1**)[29] was found to trimerize isocyanates rapidly at ambient or modest temperatures; this is remarkable since the 5-coordinate pyridyl-free analogue [Al(Salpn)(OBn)] [Salpn = bis(salicylidene)propylenediamine][30] was found to be unable to trimerize isocyanates, even under forcing conditions.§ The high activity of **3** is surprising, since a coordinatively-saturated complex is expected to be less active than a coordinatively-unsaturated one.

Reaction of the Salpy pro-ligand with AlMe₃ afforded [Al(Salpy)-Me] (**2**) in good yield (Scheme 2). Further reaction of **2** with alcohol/phenol afforded [Al(Salpy)(OR)] [R = Bn, CH₂Ph, (**3**) or Tol, 4-C₆H₄Me, (**4**)].

Isocyanate trimerization. The reaction of **3** with phenyl iso-cyanate (PhNCO; 500 equiv.) completely solidified within 1 h at 50 °C or 18 h at 25 °C (Table 1), corresponding to essentially quantitative conversion of the isocyanate to *N,N′,N′′*-triphenyl isocyanurate. NMR and mass spectra indicate that the crude product mixture is pure (only trimer is detected), and the bulk

[a] *School of Chemistry, Cardiff University, Main Building, Park Place, Cardiff CF10 3AT, UK. E-mail: WardBD@Cardiff.ac.uk*
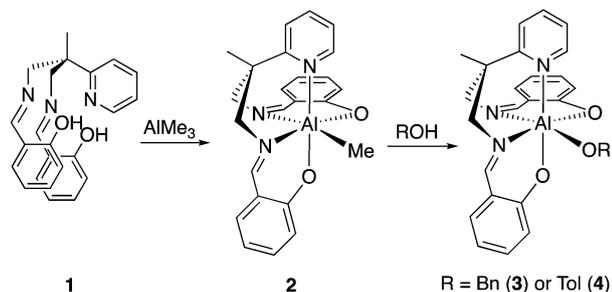[b] *Department of Science, College of Science, University of Basrah, Basrah, Iraq*
[c] *Department of Chemistry, University of Bath, Claverton Down, Bath BA2 7AY, UK*

Scheme 2 Aluminium complexes **2–4**.

product was characterized by powder X-ray diffraction (XRD). Unit cell determination and profile fitting (using the Le Bail method) led to an excellent fit to the experimental powder XRD pattern (S1.1, ESI‡). The unit cell was in excellent agreement with that of the monoclinic polymorph of the cyclotrimer reported previously.[31] Rietveld refinement of the powder XRD data confirmed that the crystalline product was the monoclinic polymorph of the cyclotrimer, from which the molecular structure of the product was confirmed (see ESI‡ for more details).[32]

From our combined analyses, we conclude that the aluminium catalyst is completely selective (within detection limits) in forming the cyclotrimer, in contrast to other catalytic systems that give various side products in addition to the isocyanurate and/or require higher catalyst loadings at higher temperatures.[17,33]

Complex **3** is active for the trimerization of alkyl, aryl and allyl isocyanates, as well as di-isocyanates (Table 1), including those of commercial relevance (especially di-isocyanates), and those that can be incorporated into polymers as cross-linking agents (e.g. allyl isocyanate).[34] From our results, it is clear that complex **3** is an exceptionally versatile catalyst, especially when considering that only low catalyst loadings are required.

Di-isocyanates find commercial use in rigid polyurethane foams and are routinely used in cavity wall, roof, and underfloor insulation. In the present work, toluene di-isocyanate

Table 1 Catalytic data for the trimerization of isocyanates and di-isocyanates by [Al(Salpy)(OBn)] (**3**)

Entry	Substrate	T (°C)	t^a (h)	Yield^b (%)
1	PhNCO	25	18	98
2	PhNCO	50	1	95
3	4-Me-C_6H_4NCO	25	48	25
4	4-Me-C_6H_4NCO	50	18	98
5	4-F-C_6H_4NCO	25	6	93
6	2-F-C_6H_4NCO	25	48	95
7	4-CF_3-C_6H_4NCO	50	18	95
8	4-Cl-C_6H_4NCO	50	0.5	97
9	4-MeO-C_6H_4NCO	50	3.5	76
10	$C_6H_5CH_2$NCO	25	3	77
11	$H_2C{=}CHCH_2$NCO	25	3	59
12	EtNCO	25	0.5	98
13	^{t}BuNCO	25	18	5
14	^{t}BuNCO	50	18	96
15	1,4-$(NCO)_2C_6H_4$ (PDI)	100^c	1.5	97
16	1,3-$(NCO)_2$-4-Me-C_6H_3 (TDI)	25	1.5	89
17	CH_2(4-NCO-C_6H_4)$_2$ (MDI)	50^c	48	90

^{a} Time taken for reaction mixture to solidify or until no further conversion attained. ^{b} Isolated yields. ^{c} Reaction carried out in the melt.

(TDI), phenylene di-isocyanate (PDI) and methylenedi(phenyl-isocyanate) (MDI) were all trimerized using complex **3** (both PDI and MDI were reacted in the melt as they are solids at room temperature). For TDI and MDI, there was clear evidence (from mass spectra) for oligomeric species arising from the reaction of both isocyanate moieties, and simple trimers were also evident. The lower intensity ν_{NCO} infrared band for the product obtained from MDI compared to those for TDI indicates a greater propensity for MDI to form higher-order oligomers.

Mechanistic aspects. The structures of **2** and **4** were confirmed by single-crystal XRD (S2.3 and S2.4, ESI‡)[35] and by elemental analysis and NMR spectroscopy. A second set of resonances was observed for **2** and **3** (but not for **4**, suggesting that the second species is present in very low concentration). In each case, several signals due to the minor component are obscured by those of the major component, but the data are consistent with the two components being isomers; the pyridyl H[6] signal for the minor isomer has a comparable chemical shift to the uncoordinated ligand (8.53 ppm for **2**; 8.58 ppm for **3**), while the pyridyl H[6] signal for the major component is further downfield (8.69 ppm for **2** and 9.10 ppm for **3**). Since the chemical shift of H[6] is indicative of the coordinative state of the pyridyl,[36] our observations suggest that the minor isomer has a de-coordinated pyridyl.

From ^{1}H NMR spectra of **3** measured between 298 K and 323 K, the equilibrium constant for the major ⇌ minor component interchange was determined at each temperature and a van't Hoff plot (S1.6, ESI‡) gave $\Delta H^{\ominus}$ = 13.6 ± 4.2 kJ mol^{-1} and $\Delta S^{\ominus}$ = 29.5 ± 13.5 J K^{-1} mol^{-1}. Hence, $\Delta G^{\ominus}$ at 298 K is estimated to be 4.8 kJ mol^{-1}. The small value of $\Delta S^{\ominus}$ is consistent with a unimolecular process rather than a monomer–dimer equilibrium, and the increase in entropy on going from the major to the minor component suggests that the major component has the coordinated pyridyl. The two components give almost identical diffusion coefficients in DOSY NMR spectra (S1.6 and Fig. S5, ESI‡).

The mechanism for the trimerization of MeNCO by [Al(Salpy)-(OMe)] (**5$_{calc}$**) was probed using DFT calculations. It is common for isocyanate trimerization to proceed via nucleophilic attack on the isocyanate carbon,[10] and there are several examples of isolated species arising from the insertion of isocyanates into metal–ligand bonds.[18,23,37–39] This leads us to propose a catalytic cycle (Scheme 3) based on a repeated coordination–insertion mechanism.¶ A crucial component of this mechanism is that pyridyl dissociation must occur before the isocyanate can associate to allow the 1,2-migratory insertion of the methoxide onto the isocyanate carbon; importantly, de-coordination of the pyridyl is facile (**S** to **INT1**: ΔG = +16 kJ mol^{-1}). Coordination of the isocyanate to the aluminium (**INT2**) is endergonic (G_{rel} = +52 kJ mol^{-1}); **INT2** lies only slightly lower in energy than the transition state **TS1** and is therefore likely to be synchronous with the insertion step.
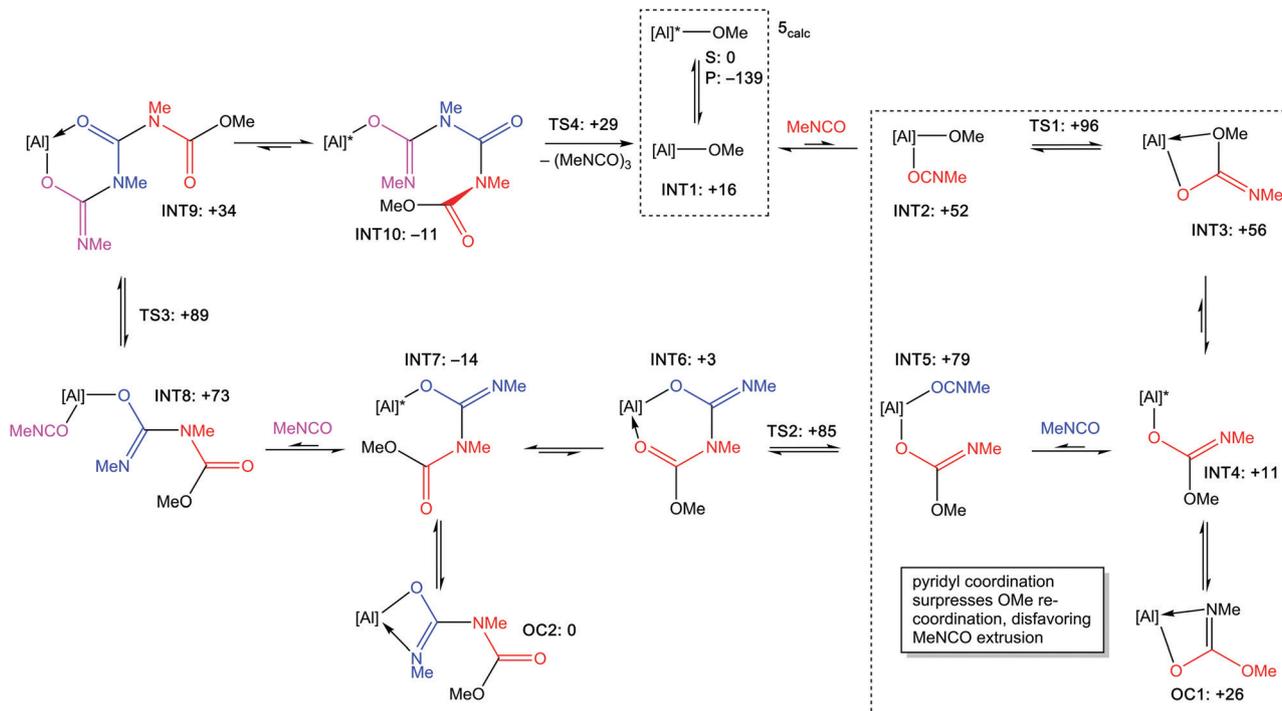
Bader's quantum theory of atoms in molecules analysis of **INT2** indicates a bond-critical point (BCP) between the associated isocyanate carbon and the methoxide oxygen, (electron density ρ = 0.09 e Å^{-3}) which indicates that the isocyanate is pre-organized for the migratory insertion of methoxide, i.e. the BCP lies along the reaction coordinate. All migratory insertion steps (**TS1** to **TS3**) can be described (natural bonding orbital analyses)

Scheme 3 Proposed catalytic cycle for the trimerization of MeNCO using [Al(Salpy)(OMe)] (5_{calc}). [Al] = [Al(κ^4-Salpy)]; [Al]* = [Al(κ^5-Salpy)]. Gibbs energies (G_{rel}) in kJ mol^{-1} calculated using M06-2X: cc-pVTZ/cc-pV(T+d)Z are shown alongside each label. The free energy profile is provided in the ESI.‡ Boxed sections highlight the pyridyl hemi-lability and its role in enhancing the catalytic activity.

as a methoxide/imine sp^2 hybrid donating to an empty p orbital of the isocyanate carbons (S3.2, ESI‡).

The product from the migratory insertion initially affords an *O,O'*-coordinated isocarbamate ligand (**INT3**), but as this is endergonic relative to **INT2**, the insertion is expected to be readily reversible without intervention of the pyridyl. However, pyridyl coordination affords a monodentate isocarbamate that has significantly lower energy (**INT4**, G_{rel} = +11 kJ mol^{-1}). Rather than re-coordination of the OMe, imine coordination is more favourable, giving **OC1** which must be an off-cycle intermediate as the imine lone pair is unavailable for the subsequent migratory insertion to isocyanate. The energetics of **INT4**, **OC1** and **INT3** support a resting state pyridyl-imine coordination equilibrium between **INT4** and **OC1**; although re-formation of **INT3** is energetically viable, an **INT4/OC1** equilibrium locks the isocarbamate into a configuration that conformationally disfavours OMe re-coordination by placing it away from the Al centre, reducing the likelihood of de-insertion and promoting the forward reaction, thus explaining the importance of the pyridyl donor in enhancing catalytic performance, consistent with experimental observations.

Insertion of subsequent isocyanates proceeds in a similar manner to the first. As the stepwise formation of an isocyanurate affords a linear series of amide linkages with rigid 120° bond angles, it follows that, after the third isocyanate insertion has taken place, the OMe group at the terminus is necessarily close to the imino nitrogen from the third isocyanate insertion, leading to cyclization to afford the isocyanurate and the regeneration of 5_{calc}. For the overall reaction, ΔG is calculated to be −139 kJ mol^{-1}.

As demonstrated in this work, the presence of a hemi-labile pyridyl donor makes the aluminium alkoxide complex [Al(Salpy)-(OBn)] (**3**) a highly active and selective catalyst for the trimerization of isocyanates under mild conditions. Calculations suggest that the pyridyl donor facilitates the partial de-coordination of the growing trimer, thereby disfavouring the de-insertion reaction. Whilst this is an important development for isocyanurate synthesis, the concept of an additional donor group enhancing catalytic performance may have profound implications for the use of labile main group metals in a wider range of catalytic reactions, and we anticipate significant research opportunities with the aim of further exploiting this concept.

Conflicts of interest

There are no conflicts to declare.

Notes and references

§ Reactions with [Al(Salpn)(OBn)] were performed at 20–100 °C for 24 hours. Isocyanurate was obtained only for 4-fluorophenylisocyanate with <15% conversion, *i.e.* with the substrate expected to have the most

electrophilic isocyanate carbon. No reaction was observed for other substrates.

¶ Stoichiometric reactions on an NMR tube scale gave rise to products consistent with a sequential insertion of isocyanates, as predicted by our hypothesized mechanism. Since, the *modus operandi* of nucleophile-based catalysts is well established, and several isolated species reported in the literature relate to isocyanate insertion into M–L bonds, there is tangible experimental verification for the validity of the mechanism shown in Scheme 3. See ESI‡ (S1.8) for full details.

1 K. V. Ragnarsdóttir, *Nat. Geosci.*, 2008, **1**, 720–721.
2 P. Gibbons, D. Love, T. Craig and C. Budke, *Vet. Parasitol.*, 2016, **218**, 1–4.
3 M. Ghosh and M. J. Miller, *J. Org. Chem.*, 1994, **59**, 1020–1026.
4 A. Bosco, L. Rinaldi, G. Cappelli, A. Saratsis, L. Nisoli and G. Cringoli, *Vet. Parasitol.*, 2015, **212**, 408–410.
5 A. P. Murray and M. J. Miller, *J. Org. Chem.*, 2003, **68**, 191–194.
6 M. Mascal, I. Yakovlev, E. B. Nikitin and J. C. Fettinger, *Angew. Chem., Int. Ed.*, 2007, **46**, 8782–8784.
7 Y. Zhang, S. N. Riduan and J. Y. Ying, *Chem. – Eur. J.*, 2009, **15**, 1077–1081.
8 E. Preis, N. Schindler, S. Adrian and U. Scherf, *ACS Macro Lett.*, 2015, **4**, 1268–1272.
9 H. Ni, A. D. Skaja, R. A. Sailer and M. D. Soucek, *Macromol. Chem. Phys.*, 2000, **201**, 722–732.
10 M. F. Sonnenschein, *Polyurethanes: science, technology, markets, and trends*, Wiley, Hoboken, New Jersey, 2015.
11 Y. Taguchi, I. Shibuya, M. Yasumoto, T. Tsuchiya and K. Yonemoto, *Bull. Chem. Soc. Jpn.*, 1990, **63**, 3486–3489.
12 Z. Pusztai, G. Vlád, A. Bodor, I. T. Horváth, H. J. Laas, R. Halpaap and F. U. Richter, *Angew. Chem., Int. Ed.*, 2006, **45**, 107–110.
13 S. M. Raders and J. G. Verkade, *J. Org. Chem.*, 2010, **75**, 5308–5311.
14 J. Tang, T. Mohan and J. G. Verkade, *J. Org. Chem.*, 1994, **59**, 4931–4938.
15 X. Liu, Y. Bai and J. G. Verkade, *J. Organomet. Chem.*, 1999, **582**, 16–24.
16 H. A. Duong, M. J. Cross and J. Louie, *Org. Lett.*, 2004, **6**, 4679–4681.
17 Y. Nambu and T. Endo, *J. Org. Chem.*, 1993, **58**, 1932–1934.
18 W. Yi, J. Zhang, L. Hong, Z. Chen and X. Zhou, *Organometallics*, 2011, **30**, 5809–5814.
19 D. Heift, Z. Benkő, H. Grützmacher, A. R. Jupp and J. M. Goicoechea, *Chem. Sci.*, 2015, **6**, 4017–4024.
20 A. Hernán-Gómez, T. D. Bradley, A. R. Kennedy, Z. Livingstone, S. D. Robertson and E. Hevia, *Chem. Commun.*, 2013, **49**, 8659–8661.
21 X. Zhu, J. Fan, Y. Wu, S. Wang, L. Zhang, G. Yang, Y. Wei, C. Yin, H. Zhu, S. Wu and H. Zhang, *Organometallics*, 2009, **28**, 3882–3888.
22 Y. Wu, S. Wang, X. Zhu, G. Yang, Y. Wei, L. Zhang and H. Song, *Inorg. Chem.*, 2008, **47**, 5503–5511.
23 X. Zhou, L. Zhang, M. Zhu, R. Cai, L. Weng, Z. Huang and Q. Wu, *Organometallics*, 2001, **20**, 5700–5706.
24 H. R. Sharpe, A. M. Geer, H. E. L. Williams, T. J. Blundell, W. Lewis, A. J. Blake and D. L. Kays, *Chem. Commun.*, 2017, **53**, 937–940.
25 A. J. Bloodworth and A. G. Davies, *J. Chem. Soc.*, 1965, 6858–6863.
26 F. Moghaddam, M. Dekamin and G. Koozehgari, *Lett. Org. Chem.*, 2005, **2**, 734–738.
27 A. Flamini, A. M. Giuliani and N. Poli, *Tetrahedron Lett.*, 1987, **28**, 2169–2170.
28 S. G. Lee, K.-Y. Choi, Y.-J. Kim, S. Park and S. W. Lee, *Dalton Trans.*, 2015, **44**, 6537–6545.
29 R. Shakya, A. Jozwiuk, D. R. Powell and R. P. Houser, *Inorg. Chem.*, 2009, **48**, 4083–4088.
30 H. Du, X. Pang, H. Yu, X. Zhuang, X. Chen, D. Cui, X. Wang and X. Jing, *Macromolecules*, 2007, **40**, 1904–1913.
31 A. Usanmaz, *Acta Crystallogr., Sect. B: Struct. Crystallogr. Cryst. Chem.*, 1979, **35**, 1117–1119.
32 K. D. M. Harris, *Advanced X-Ray Crystallography*, Springer, Berlin, Heidelberg, 2012, vol. 315, pp. 133–177.
33 F. Paul, S. Moulin, O. Piechaczyk, P. Le Floch and J. A. Osborn, *J. Am. Chem. Soc.*, 2007, **129**, 7294–7304.
34 W. Sun, X. Yan and X. Zhu, *J. Appl. Polym. Sci.*, 2011, **122**, 2359–2367.
35 S. J. Coles and P. A. Gale, *Chem. Sci.*, 2012, **3**, 683–689.
36 S. Friedrich, M. Schubart, L. H. Gade, I. J. Scowen, A. J. Edwards and M. McPartlin, *Chem. Ber./Recl.*, 1997, **130**, 1751–1759.
37 L. Orzechowski and S. Harder, *Organometallics*, 2007, **26**, 2144–2148.
38 H. Wang, H.-W. Li and Z. Xie, *Organometallics*, 2003, **22**, 4522–4531.
39 W. Uhl, J. S. Bruchhage, M. Willeke, A. Hepp and J. Kösters, *Eur. J. Inorg. Chem.*, 2016, 2721–2730.